LARGE EDDY SIMULATIONS FOR THERMAL FATIGUE PREDICTIONS IN A T-JUNCTION: WALL-FUNCTION OR WALL-RESOLVE BASED LES?

S.T. Jayaraju[1], E.M.J. Komen[1] and E. Baglietto[2]

[1]Nuclear Research & Consultancy group, P.O. Box 25, 1755 ZG Petten, The Netherlands
[2]CD-Adapco, Nuclear Applications, 60 Broadhollow Rd, Melville, New York

Abstract

Large Eddy Simulations are performed in a T-junction to analyze the feasibility of wall-functions in accurately predicting the thermal fluctuations acting on the pipe walls. The WALE sub-grid-scale model employed in the LES solver is validated by performing OECD/NEA T-Junction benchmark test-case. In order to reduce the computational costs, Reynolds number scaling is performed while preserving the essential flow features. While the wall-function based simulation showed good agreement with the wall-resolved approach for the bulk velocity and temperature field, the corresponding RMS components were consistently under-estimated close to the wall boundaries. The same was true for the RMS fluctuations of the wall heat-flux. As a consequence, it is concluded that any similarity in the bulk profiles does not guarantee any kind of similarity in the wall heat flux behavior.

1. INTRODUCTION

Thermal fatigue is a degradation mechanism induced on the primary piping system of a nuclear power plant. Consequences of thermal fatigue are often very critical, ranging from structural damage to a complete shut-down as happened with the French pressurized water reactor (PWR) Civaux in 1998 (Peniguel et al., 2003). Thermal fatigue has been a very persistent problem and has also occurred in the Japanese PWR Tsuruga-2 in 1999, and the Japanese PWR Tomari-2 in 2003. Hence, it is considered to be a serious safety concern and is seen as one of the most influential parameters on the ageing and life management of nuclear power plants (Walker et al., 2009).

The mixing of hot and cold flow streams causes high cycle temperature fluctuations next to piping walls. The temperature fluctuation leads to stress fluctuations. These fluctuating stresses acting on the piping system is one of the potential causes for thermal fatigue. Such a situation occurs outside of the nuclear core region, which typically involves piping systems such as Tjunctions, elbows and leakage valves. In particular, the mixing T-junctions of the residual heat removal systems in the reactors are seen to be most susceptible to thermal striping (Hu and Kazimi, 2006). The present work is related to Computational Fluid Dynamics (CFD) analysis of turbulent mixing in one such T-junction aiming to understand the suitability of wall-functions (WF) in predicting the near-wall flow characteristics and heat transfer to the wall in comparison to a more computationally expensive wall-resolved (WR) approach.

CFD has emerged to be an effective tool to study the thermal fatigue phenomena. The most widely used Reynolds Averaged Navier Stokes (RANS) methodology exhibits difficulties in accurately predicting such flows (Westin et al., 2008; Manera et al., 2009). Recent studies have moved to more advanced numerical tools such as Large Eddy Simulation (LES) and Detached Eddy Simulation (DES). Most of the studies which involve LES simulations, wall-functions have been used.

For any accurate CFD analysis of thermal fatigue, it is very important that the thermal fluctuations on the walls of the mixing tee are accurately predicted. The standard wall-function based LES simulation in a T-junction performed by Pasutto et al. (2005) has shown that the temperature fluctuations next to the walls are strongly attenuated, leading to large

error in wall temperature fluctuation predictions when compared to the experiments. Employing the wall-function based LES approach; Howard and Pasutto (2009) also highlight the importance of evaluating how accurate the wall modeling approaches are. The DES simulations of Westin et al. (2008) and Nakamura and Oumaya (2009) also raise the same question about the accuracy of near-wall modeling. Based on these observations, we recognize the near-wall modeling as a very important and critical aspect that influences the accuracy of any CFD prediction. Hence, in the present work, we made it an objective to test the feasibility of using wall-functions to accurately predicting the near-wall flow characteristics and heat transfer to the wall.

2. APPROACH TO REACH THE OBJECTIVE

2.1. Solver selection

Selecting an appropriate CFD solver which has the capabilities to handle complex meshes and possesses efficient numerical solvers to obtain accurate results is of primary importance. The present work has been carried out employing STAR-CCM+ (STAR-CCM+, 2009). STAR-CCM+ is a finite volume multi-physics solver with capabilities of creating good quality arbitrary hexahedral and polyhedral meshes on complex geometries. Creating a high quality wall-resolved mesh which meets the LES requirements (Piomelli, 1997) is far from simple, especially when the computational domain involves sharp 90 degree joints. In the present T-junction case, such a sharp angle exists in the junction between two pipes. STAR-CCM+ meshing tool is equipped with advanced methodologies to treat such corners. In terms of the numerical solver, STAR-CCM+ uses advanced cell-based discretization techniques and sophisticated Algebraic-Multi-Grid (AMG) strategies for convergence acceleration. Based on all these advantages, STAR-CCM+ has been chosen to be one of the most efficient solvers for the present work.

2.2. Solver validation

The LES solver of STAR-CCM+ has been validated by simulating OECD/NEA benchmark experiments very recently performed in 2010. Fig. 1 shows a schematic representation of the computational domain.

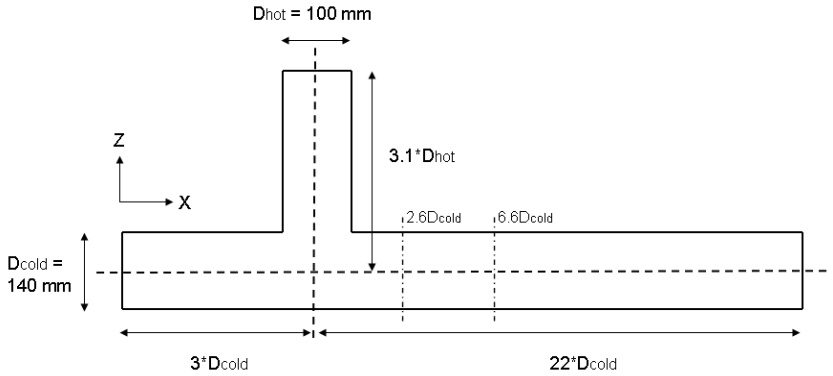

Figure 1: Schematic representation of the computational domain

The geometry consists of two perpendicularly connected circular pipes which form the T-junction. The cold and hot inlet diameters were 140mm and 100mm respectively. The experiments were performed with a cold inlet flow rate of 9 l/s and hot inlet flow rate of 6 l/s. The temperature differences between cold and hot inlet was set to 17K with cold inlet at 292K and hot inlet at 309K. The geometrical model was manufactured in plexiglass, and this is an adiabatic test-case. The velocity profiles in the inlet pipes and downstream of the T-junction

were measured using Laser Doppler Velocimetry (LDV). Temperature fluctuations on the pipe walls have been measured by placing thermo-couples at several locations downstream of the T-junction. All thermo-couples are placed at approximately 1mm below the pipe walls. Detailed CFD validation results of this case are presented in Section 4.1.

2.3. Original vs. scaled Reynolds number

Performing a non-adiabatic wall-resolved LES simulation at Reynolds number equivalent to that of experiments described in the previous section is computationally very expensive. Within the experimental work performed by Andersson et al. (2006), two additional tests were performed by scaling down and scaling up the flow rate by a factor of 2. The results showed weak dependence of flow characteristics on the flow rate. These results prompted us to go down in the Reynolds number by linearly scaling down the inlet flow-rates. The primary aim of such a scaling is to reduce the computational costs required for LES.

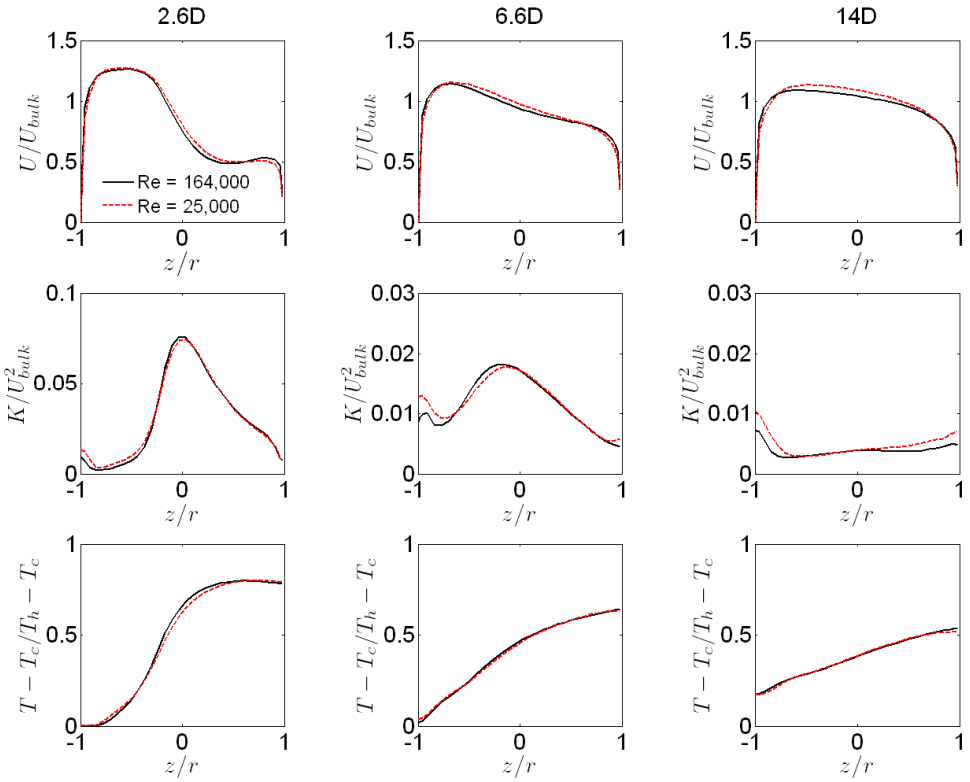

Figure 2: Comparison of normalized velocity magnitude, kinetic energy and temperature at 2.6 diameters (left column), 6.6 diameters (middle column) and 14 diameters (right column) downstream of the mixing zone.

One of the main criteria for scaling down was to ensure that the solution at scaled down Reynolds number was representative of the solution at original Reynolds number. This was tested by performing steady-state RANS simulations at two different Reynolds numbers of 162 918 and 24 500. Realizable k − ε turbulence model (Shih et al., 1994) along with wall-functions (Reichardt, 2003) were used. Comparison of normalized flow characteristic profiles at three different diameters downstream of mixing zone are as shown in Fig. 2. As can be seen, the profiles at Reynolds number of 24 500 show very similar trend when compared to the profiles at Reynolds number 162 918. There are visibly small differences in the kinetic energy predictions close to the walls, however, the overall patterns at these two Reynolds numbers match each other. This result gave further confidence that the flow patterns at Re 24

500 are representative of the flow patterns that occur at a much higher Reynolds number of 162 918.

2.4. Selection of wall-temperature for non-adiabatic case

In the actual thermal fatigue scenario, the mixing of hot and cold fluid in a T-junction generates temperature fluctuations next to the walls and there is always some heat transfer across the boundary. Such a scenario can be replicated computationally in two ways. One is by fixing the wall temperature and letting the heat-flux vary across the boundary, and the second is to prescribe a fixed heat-flux on the walls and let the wall temperature vary accordingly. In the present work, we decided to fix the wall temperature to a constant value and let the heat-flux vary. The next step was to decide what wall temperature to fix. At the scaled Reynolds number of 24 500, four different RANS simulations with wall temperatures of 283K, 273K, 243K and 200K respectively were performed. 243K was finally chosen as it provided significant temperature gradients in the bulk of flow domain. Even though the value of 243K has no physical meaning in the context of reality, it was selected because the main objective here was to test the applicability of wall functions when there is significant temperature gradient in the bulk flow downstream of the mixing zone.

2.5. Summary of three LES cases

The three main LES simulations performed in the present work are summarized in Table 1. Case 1 is the solver validation case which is adiabatic. Case 2 and 3 are non-adiabatic simulations with and without wall-functions respectively.

Table 1: Description of 3 LES cases

Case No.	Q_{cold} (l/s)	Q_{hot} (l/s)	Re	T_{wall} (K)	T_{cold} (K)	T_{hot} (K)	WF/WR
1	9	6	152780	Adiabatic	292.15	309.15	WF
2	1.80456	0.90228	24 500	243.15	288.15	303.15	WF
3	1.80456	0.90228	24 500	243.15	288.15	303.15	WR

3. CFD ASPECTS

3.1. Computational mesh

The mesh at the inlet cross-section as shown in Fig. 3 gives an idea of the kind of mesh distribution for the three cases. The grids were created based on the Piomelli (1997) guidelines. The three different grid parameters are as summarized in Table 2.

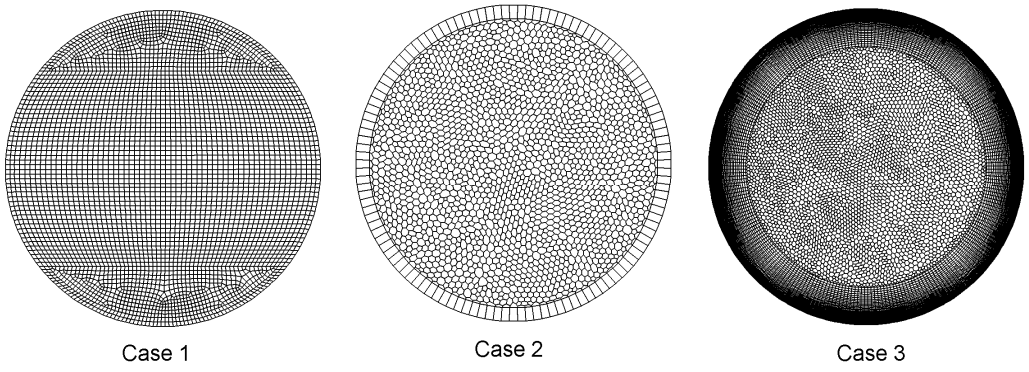

Figure 3: Computational mesh at the cold inlet surface for 3 cases

Table 2: Description Grid specifications for 3 LES cases

Case No.	Re	WF/WR	Δ^+_{axial}	$\Delta^+_{circumferencial}$	$\Delta^+_{wall-normal}$	Mesh Size
1	152780	WF	100	100	100	13 220 000
2	24 500	WF	100	30	60	919 317
3	24 500	WR	100	20	1	7 016 966

3.2. Main fluid-dynamics model

This is a three-dimensional, incompressible, Large Eddy Simulation. Constant fluid properties are assumed for all three LES cases. Please note that for Case 2 and 3, there are large temperature differences within the domain. This will surely affect the fluid properties and our assumption of constant fluid properties is not valid. However, since we are aiming to perform one to one comparison between Case 2 and 3, assuming constant fluid properties will not have any effect on our final objective.

3.3. LES model

The two Sub-Grid-Scale (SGS) models available within STAR-CCM+ are the Smagorinsky model (Smagorinsky, 1963) and theWALE model (Nicoud and Ducros, 1999). In the present work, the WALE model is employed because of its obvious advantages over Smagornisky. The WALE model is specifically designed to return the correct wall-asymptotic y^3 behavior of the SGS viscosity. The model is based on the square of the velocity gradient tensor and accounts for the effect of both the strain and the rotation rate to obtain the local eddy viscosity. The WALE model unlike the Smagorinsky model needs neither a damping function nor a dynamic procedure to account for the no-slip condition at the walls (Jayaraju et al., 2008). Above this, the validations performed using the WALE model shows seemingly less sensitiveness to the value of the model coefficient than the Smagorinsky model (STAR-CCM+, 2009).

Similar to the experiments, the temperature equation is simulated as a passive scalar for all three LES cases. For the Case 1 and 2, velocity wall- functions are based on Reichardt (2003), and the temperature wall-functions are based on Kader (1981).

3.4. Physical properties

The physical properties of the working fluid for all three LES cases are as given in Table 3.

Table 3: Physical properties of the working fluid

Density (kg/m^3)	Dynamic viscosity (kg/m-s)	Specific heat (J/kg-K)	Thermal conductivity (W/m-K)	Molecular Prandtl No.	Turbulent Prandtl No.
998.2	1e-3	4182	0.6	7	0.85

3.5. Boundary conditions

For Case 1, inlet profiles based on the experimental measurements (Andersson et al., 2006) are applied at both cold and hot inlet. Static atmospheric pressure is considered at the outlet. For the details of flow-rates and temperature values, please refer to Table 1. For Case 2 and 3, the inlet profiles are scaled down linearly to match the desired Reynolds number. Kuczaj et al. (2008) performed few test simulations and found that the main generation of turbulence is caused by the mixing process of two fluids and the inlet turbulence levels are of no importance. The same has also been observed by Westin et al. (2008) and Odemark et al. (2009). Hence, no perturbations are applied at the inlet boundaries.

3.6. Initial field

A steady-state RANS simulation is performed and used as an initial guess to start LES for all three cases.

3.7. Numerical aspects

A stable blend of central and upwind schemes, called as the bounded central differencing is used for spatial discretization of the momentum equation. A blending factor of 0.1 is used in the present work. The bounded central scheme is activated only when the solver detects face fluxes which generate local extrema. In all other circumstances, the scheme behaves as a purely central differencing. A second order implicit formulation is employed for temporal discretization. As an accuracy requirement, the physical time-step was chosen in such a way that the average Courant number in the domain is around 1. This results in a physical time-step of Δt = 5e-4 sec for Case 1, and Δ = 5e-3 sec for Case 2 and 3. Please note that Case 2 being a WF based simulation could have afforded a bigger time-step than Case 3, however, for the sake of consistency, the time-step was kept identical for both Case 2 and 3. To get rid of any possible initial condition effects, two time-periods of flow were simulated before starting the time-averaging. To obtain a smooth time-averaging, 6 time periods were simulated. A time period is defined as the ratio of geometrical length of the T-junction to the inlet bulk velocity.

4. RESULTS

4.1. Solver validation

The Case 1 simulation results, which are intended for STAR-CCM+ LES solver validation are presented in this section by comparing cross-sectional 2D plots of velocity and temperature at different locations in the geometry. Fig. 4 shows the comparison of mean and RMS velocity components between experiments and LES. The results displayed include streamwise and spanwise velocity components at 2.6 diameters downstream of the mixing zone. This location is where most gradients in the flow exist and are generally more difficult to capture. As seen in Fig. 4, there is an overall good agreement between experiments and CFD predictions.

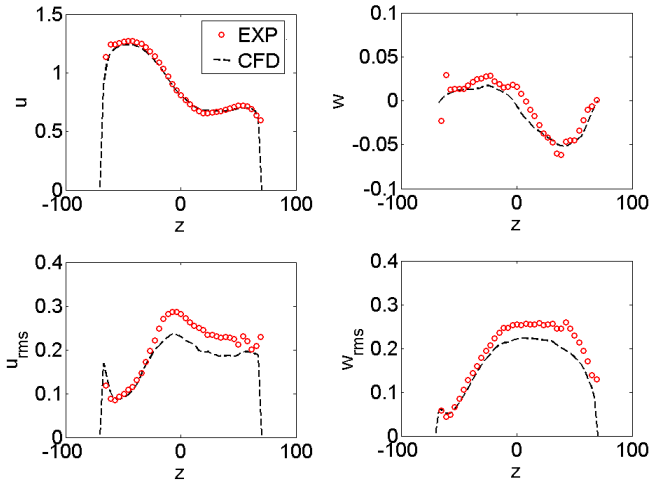

Figure 4: Comparison of the mean and RMS velocity profiles at 2.6 diameters downstream of the mixing zone

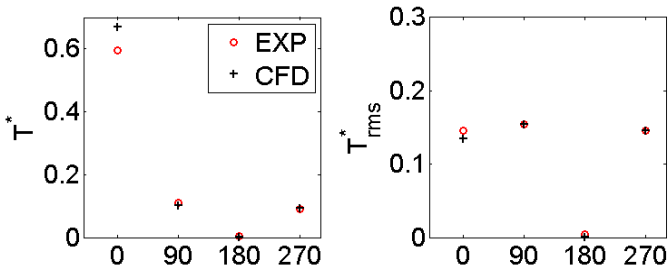

Figure 5: Comparison of the normalized mean and RMS temperatures at 4 different angular positions which are located at 2.6 diameters downstream of the mixing zone.

Fig. 5 shows the comparison of normalized mean ($T-T_c/T_h-T_c$) and normalized RMS (T_{rms}/T_h-T_c) temperature at 4 different thermocouple locations placed at 2.6 diameters downstream of the mixing zone. Overall, there is good agreement between experiments and CFD predictions for both mean and RMS quantities. Based on these results, we conclude that the LES solver of STAR-CCM+ has good predictive capabilities.

4.2. Wall-function vs. wall-resolved for scaled Reynolds number

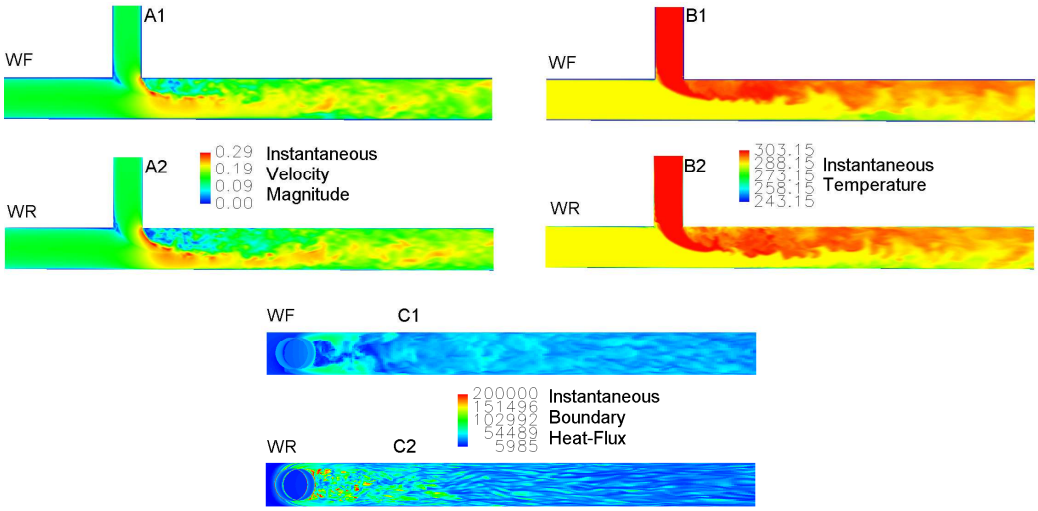

Figure 6: Instantaneous flow profiles for the wall-function (WF) and wall-resolved (WR) approach. A1,A2: Instantaneous velocity magnitude at the center cut plane. B1,B2: Instantaneous temperature at the center cut plane. C1,C2: Instantaneous heat-flux on pipe walls.

In the present section, the non-adiabatic simulations performed using wall function approach (Case 2) and the wall-resolved approach (Case 3) are compared in detail. In order to have a global impression of the flow characteristics in the T-junction, we look at the contours of instantaneous flow parameters as shown in Fig. 6. From the instantaneous velocity magnitude contours (Fig. 6A1,A2), it is seen that the flow entering from two perpendicular pipes start to mix in the junction resulting in a jet like structure developing towards the lower wall of the pipe. Because of this high velocity skewed jet, a recirculation zone is formed on the upper pipe wall which spans till 2 to 3 diameters downstream of mixing zone. The cross-sectional mean axial velocity plots in Fig. 7 indeed shows that the skewed velocity profiles prevail until 4 diameters, beyond which they smooth out to become more flatter as a result of enhanced mixing. The instantaneous temperature contours (Fig. 6B1,B2) show that the cold fluid entering from the left and the hot fluid from the top starts to mix at the junction, and as we go further downstream, the temperature distribution becomes more uniform as expected. For the wall heat-flux predictions (Fig. 6C1,C2), substantial qualitative as well as quantitative

differences are seen between WF and WR approach. One apparent observation is the presence of low-flux streaks in the wall resolved simulation, which are completely not captured by the wall-function approach.

To quantify the predictive capabilities of the WF approach, we look at the cross-sectional comparison of flow parameters as shown in Fig. 7. It is clear that the simulated mean axial velocity and mean temperature profiles in the bulk for the WF approach are in close agreement with that of the WR approach. This highlights the predictive capabilities of wall-functions in the bulk region of the flow domain. While the mean flow parameters show promising results, the RMS velocity and RMS temperature predictions indicate that the WF approach consistently under-estimates the fluctuations near the boundaries. Especially, the RMS temperature profiles from the WR approach show very large gradients close to the walls which are not captured by the WF approach throughout the stream-wise direction. This is simply because of the fact that the largest gradients are existing in the y+ range well below 30 and the first grid point for the WF based grid is placed at around y+ 30. This implies that the WF grid simply cannot see any gradients below y+ around 30. These differences in RMS temperature predictions can have considerable effect on the heat transfer happening across the pipe walls. The differences in the instantaneous wall heat-flux contours for WF and WR approach (Fig. 6C1,C2) already gives a qualitative picture of the differences. The thin stream-wise streaky structures seen in the WR approach (Fig. 6C2) are not observed in the WF approach (Fig. 6C1). While performing a channel flow simulation, Hadziabdic (2004) highlights the importance of capturing such longitudinal streaky structures in accurately predicting the mean and RMS quantities.

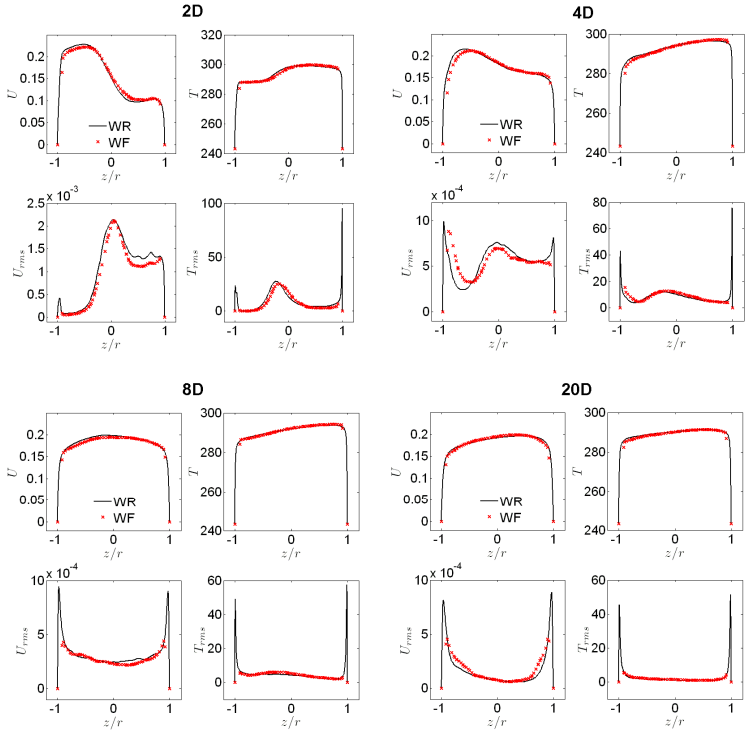

Figure 7: Mean and RMS component comparison of flow variables at 2, 4, 8 and 20 diameters downstream of the mixing zone.

The quantitative differences in the mean and RMS wall heat-flux predictions for the WF and WR approach are shown in Fig. 8. While Fig. 8A,C represents the mean and RMS heat-flux from 0.5 to 8 diameters downstream of mixing zone, Fig. 8B,D represents the same from 14 to 20 diameters downstream. Since large values of heat-flux are seen towards the top wall

region, the present plots are extracted at the top wall side. The WF approach under-estimates the mean heat-flux prediction up to approximately 4 diameters (Fig. 8A), beyond which it is slightly over-estimated. A considerable over-estimation of mean heat-flux in case of the WF approach is also observed from 14 to 20D. At the first glance, this over-prediction may seem to be contra-intuitive as one expects the differences between WF and WR approach to reduce as we go far downstream, simply because the flow moves towards attaining fully developed state. Generally speaking, the wall-functions can be expected to perform well, at least for the mean flow quantities, if the flow is fully developed. However, for the present Reynolds number, it would take anywhere between 20 to 50 diameters to have a fully developed flow. This may explain the differences in mean heat-flux predictions between WF and WR approach even at 14 to 20 diameters downstream.

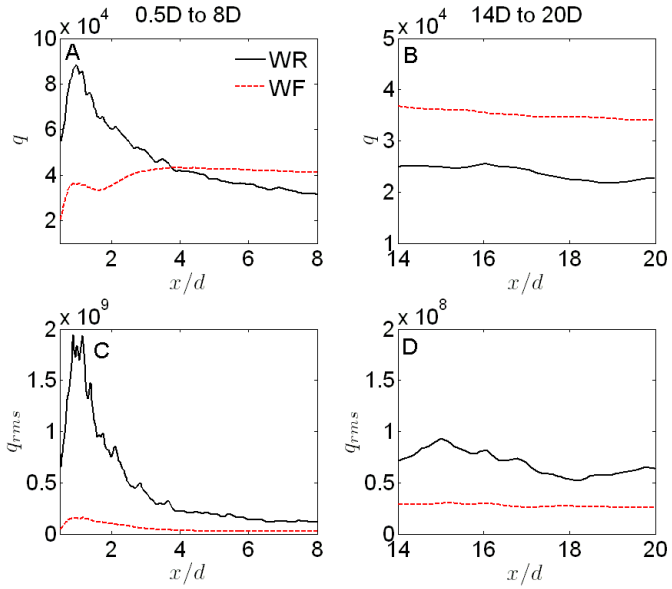

Figure 8: Mean and RMS wall heat-flux predictions. A,C: From 0.5 to 8 diameters along the wall. B,D: From 14 to 20 diameters along the wall.

The RMS heat-flux is consistently under-estimated from 0.5 to 8 diameters as well as from 14 to 20 diameters (Fig. 8C,D). As the heat flux is directly proportional to the temperature gradient, the under-estimation of RMS tem perature close to the walls results in the under estimated RMS heat-flux. The maximum fluctuations of heat-flux are observed at approximately 1 diameter downstream of the mixing zone. It is a known fact that the thermal fatigue occurs very close to the mixing zone and the under-prediction of RMS heat flux in this vicinity raises a concern over the applicability of wall-functions. It is interesting to note that the standard wall-function based LES simulation in a T-junction performed by Pasutto et al. (2005) has also shown that the temperature fluctuations next to the walls are strongly attenuated, leading to a large error in wall temperature fluctuation predictions when compared to the experiments.

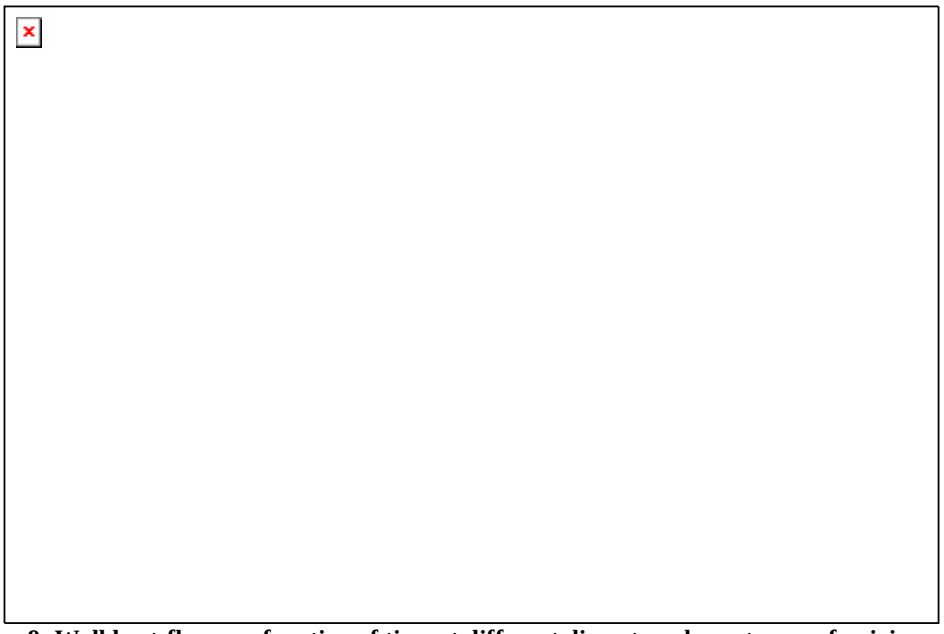

Figure 9: Wall heat-flux as a function of time at different diameters downstream of mixing zone.

Fig. 9 shows the time evolution of heat-flux at different locations on the wall. For the WR approach, the amplitude of the signal is always higher than the WF approach at all 5 locations considered. This explains the under prediction of RMS heat-flux throughout the domain (Fig. 8C,D). The overestimation of the mean heat-flux between 14D to 20D (Fig. 8B) can directly be noticed in the time variant heat-flux plot (Fig. 9D,E).

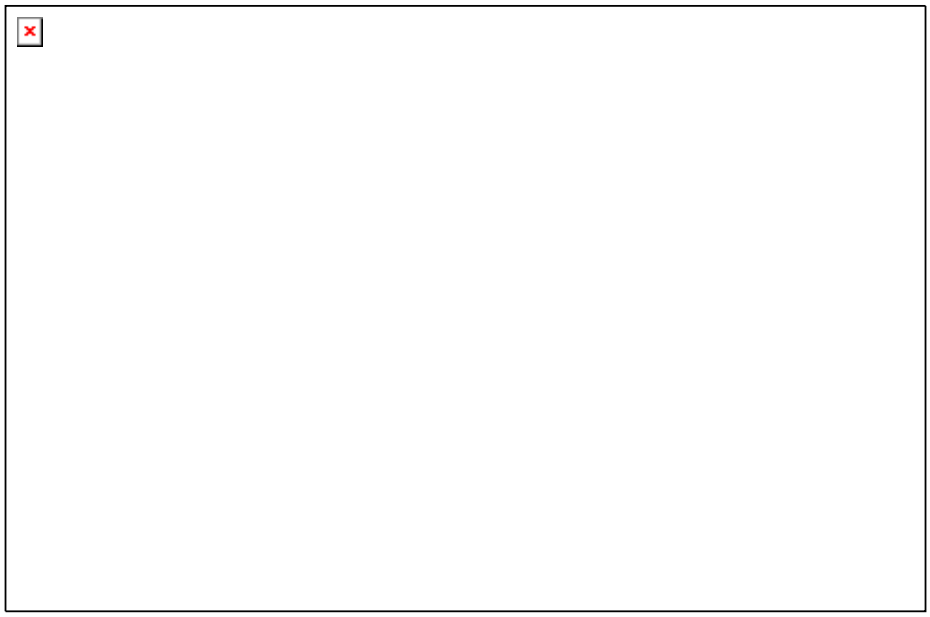

Figure 10: Wall heat-flux spectra at different diameters downstream of the mixing zone.

Thermal fatigue is a phenomenon which has a significant impact only in certain frequency range of loading where rapid propagation of macroscopic cracks occur. The thermal fatigue analysis in a T-junction by Chapuliot et al. (2005) indicates the range of effective frequencies to be between 0.1Hz to 10Hz. Hence, analyzing the heat-flux spectrum in this frequency range will provide more insights regarding the suitability of wall-functions. Fig. 10 shows the spectrum of the heat flux recorded on the wall at different axial locations. The sampling

frequency of the signal was 200Hz for both WF and WR approach. At one diameter downstream, there is approximately an order of magnitude difference between the WF and WR spectrum (Fig. 10A). The differences tend to reduce as we go further downstream. As already mentioned, thermal fatigue generally occurs in the close range of mixing zone. Hence, in the range of our interest (1D to 4D), there are substantial differences between the WF and WR approach which raises doubts regarding the applicability of wall-functions for the considered application.

While the results presented here shows that the applicability of wall-functions are questionable, a conclusive answer warrants further investigations which are closer to reality. The present work assumes a constant wall temperature and let the heat-flux vary accordingly. In actual thermal fatigue scenario's, there is conjugate heat-transfer between the fluid and the solid walls. In future, analyzing the wall temperature fluctuations by performing conjugate heat-transfer simulations with fluid-structure thermal interaction would bring more insights to the wall-function applicability.

5. CONCLUSIONS

Non-adiabatic LES simulations are performed in a T-junction to study the suitability of wall-functions in accurately predicting the thermal fluctuations on the pipe walls. The main conclusions of this work are summarized as follows:

1. It was possible to perform Reynolds number scaling while preserving the essential mean flow features, in order to reduce the computational costs incurred by challenging LES simulations.

2. The WALE sub-grid-scale model showed good predictive capabilities of the bulk mixing in the considered adiabatic experimental test case.

3. In the bulk region of the flow, the time-averaged mean velocity and mean temperature profiles were consistently captured by WF approach when compared with that of WR approach.

4. The time-averaged RMS velocity and RMS temperature profiles show large gradients close to the walls in case of the WR simulations. The WF approach on other hand severely under-estimates these gradients.

5. On the pipe walls, the WF approach consistently under-estimates the RMS heat-flux throughout the stream-wise direction of the domain.

6. For the relevant frequency range (0.1 to 10Hz) and the spatial location range (1D to 4D) of interest for thermal fatigue, there are substantial differences in the wall heat-flux spectrum.

REFERENCES

Andersson, U., Westin, J., Eriksson, J., 2006. Thermal mixing in a t-junction. Technical report u 06:66, Vattenfall research and development AB.

Chapuliot, S., Gourdin, C., Payen, T., Magnaud, J. P., Monavon, A., 2005. Hydro-thermal-mechanical analysis of thermal fatigue in a mixing tee. Nuclear Engineering and Design 235, 575 – 596.

Hadziabdic, M., 2004. Les, RANS and combined simulation of impinging flows and heat transfer. Ph.D. thesis, University of Sarajevo, Bosnia and Herzegovnia.

Howard, R. J. A., Pasutto, T., 2009. The effect of adiabatic and conducting wall boundary conditions on LES of a thermal mixing tee. NURETH-13.

Hu, L. W., Kazimi, M. S., 2006. LES benchmark study of high cycle temperature fluctuations caused by thermal striping in a mixing tee. International Journal of Heat and Fluid Flow 27, 54 – 64.

Jayaraju, S. T., Brouns, M., Lacor, C., Belkassem, B., Verbanck, S., 2008. Large eddy and detached eddy simulations of fluid flow and particle deposition in a human mouththroat. Journal of Aerosol Science 39, 862–875.

Kader, B. A., 1981. Temerature and concentration profiles in fully turbulent boundary layers. International Journal of Heat and Mass Transfer 24, 1541-1544.

Kuczaj, A. K., de Jager, B., Komen, E. M. J., 2008. An assessment of large eddy simulation for thermal fatigue prediction. International Congress on Advances in Nuclear Power Plants.

Manera, A., Prasser, H., Lechner, R., Frank, T., 2009. Towards the prediction of temperature fluctuations by means of steady RANS for the estimation of thermal fatigue. NURETH-13.

Nakamura, A., Oumaya, T., 2009. Numerical investigation of thermal stripping at a mixing tee using des. NURETH-13.

Nicoud, F., Ducros, F., 1999. Subgrid-scale stress modelling based on the square of the velocity gradient tensor. Flow Turbulence and Combustion 62-3, 183–200.

Odemark, Y., Green, T. M., Angele, K., Westin, J., Alavyoon, F., Lundstrom, S., 2009. High-cycle thermal fatigue in mixing tees: new LES validated against new data obtained by piv in the vattenfall experiments. ICONE-17.

Pasutto, T., Peniguel, C., Sakiz, M., 2005. Chained computations using an unsteady 3d approach for the determination of thermal fatigue in a tjunction of a pwr nuclear plant. International Congress on Advances in Nuclear Power Plants.

Peniguel, C., Sakiz, M., Benhamadouche, S., Stephan, J. M., Vindeirinho, C., 2003. Presentation of a numerical 3d approach to tackle thermal striping in a PWR nuclear t junction. ASME PVP.

Piomelli, U., 1997. Large eddy and direct numerical simulations of turbulent flows. Lecture notes.

Reichardt, H., 2003. Vollstaendige darstellung der turbulenten geschwindigkeitsverteilung in glatten leitungen. S. Angew. Math. Mech 31(7), 208 – 219.

Shih, T. H., Liou, W. W., Shabbir, A., Yang, Z., Zhu, J., 1994. A new k − ε eddy viscosity model for high Reynolds number turbulent flows. NASA TM 106721.

Smagorinsky, J., 1963. General circulation experiments with the primitive equation. Monthly Weather Report 91-3, 99–106.

STAR-CCM+, 2009. User manual, version 4.04.011. CD Adapco, London.

Walker, C., Simiano, M., Zboray, R., Prasser, H. M., 2009. Investigations on mixing phenomena in single-phase flow in a t-junction geometry. Nuclear Engineering and Design 239, 116 – 126.

Westin, J., Mannetje, C., Alavyoon, F., Veber, P., Andersson, L., Andersson, U., Eriksson, J., Henriksson, M., Andersson, C., 2008. High-cycle thermal fatigue in mixing tees. large eddy simulations compared to a new validation experiment. ICONE16.